

RANKL Inhibition Through Osteoprotegerin Blocks Bone Loss in Experimental Periodontitis

Qiming Jin,* Joni A. Cirelli,* Chan Ho Park,*† James V. Sugai,* Mario Taba Jr.,* Paul J. Kostenuik,‡ and William V. Giannobile*†§

Background: Prevention of alveolar bone destruction is a clinical challenge in periodontal disease treatment. The receptor activator of nuclear factor-kappa B ligand (RANKL) inhibitor osteoprotegerin (OPG) inhibits osteoclastogenesis and suppresses bone resorption.

Methods: To study the effects of RANKL inhibition on alveolar bone loss, an experimental ligature-induced model of periodontitis was used. A total of 32 rats were administered human OPG-Fc fusion protein (10 mg/kg) or vehicle by subcutaneous delivery twice weekly for 6 weeks. Negative or positive controls received no treatment or disease through vehicle delivery, respectively. Biopsies were harvested after 3 and 6 weeks, and mandibulae were evaluated by microcomputed tomography (μ CT) and histology. Serum levels of human OPG-Fc and tartrate-resistant acid phosphatase-5b (TRAP-5b) were measured throughout the study by enzyme-linked immunosorbent assay (ELISA). Statistical analyses included analysis of variance (ANOVA) and Tukey tests.

Results: Human OPG-Fc was detected in the sera of OPG-Fc-treated animals by 3 days and throughout the study. Serum TRAP-5b was sharply decreased by OPG-Fc treatment soon after OPG-Fc delivery and remained low for the observation period. Significant preservation of alveolar bone volume was observed among OPG-Fc-treated animals compared to the controls at weeks 3 and 6 ($P < 0.05$). Descriptive histology revealed that OPG-Fc significantly suppressed osteoclast surface area at the alveolar crest.

Conclusion: Systemic delivery of OPG-Fc inhibits alveolar bone resorption in experimental periodontitis, suggesting that RANKL inhibition may represent an important therapeutic strategy for the prevention of progressive alveolar bone loss. *J Periodontol* 2007;78:1300-1308.

KEY WORDS

Bone resorption; osteoprotegerin; periodontal disease; receptor activator of nuclear factor-kappa B ligand; therapy.

Periodontitis is a destructive disease that targets tooth-supporting structures through complex and multifactorial pathogenic processes. It is triggered by an interaction between bacterial components of tooth-associated biofilms and host response mechanisms.¹ Alveolar bone destruction, a hallmark of periodontitis progression and one of the major causes of tooth loss in humans, is mediated by the host immune and inflammatory response to microbial challenge. In recent decades, studies on cellular and molecular mechanisms of bone loss in periodontitis have suggested that the use of host modulation agents is an important adjunctive therapy to antimicrobial strategies.²

The discovery of the receptor activator of nuclear factor-kappa B (RANK)/RANK ligand (RANKL)/osteoprotegerin (OPG) axis has improved the knowledge of bone metabolism regulation and created a new field for the study of treatment of bone destruction-related diseases, including rheumatoid arthritis, metastatic bone cancer, and periodontal disease. The RANKL/RANK interaction is needed for differentiation and maturation of osteoclast precursor cells to activated osteoclasts and for the survival of mature osteoclasts. Stimulatory factors such as hormones (vitamin D₃, parathyroid hormone, parathyroid hormone-related protein), cytokines (interleukin-1, -6, -11, and -17), growth factors (tumor necrosis

* Department of Periodontics and Oral Medicine, School of Dentistry, University of Michigan, Ann Arbor, MI.

† Department of Biomedical Engineering, College of Engineering, University of Michigan.

‡ Metabolic Disorders Research, Amgen, Thousand Oaks, CA.

§ Michigan Center for Oral Health Research, Ann Arbor, MI.

factor- α and bone morphogenetic protein-2), and other molecules (prostaglandin E_2 , cytoplasmic domain-40L, and glucocorticoid), upregulate the expression of the RANKL gene in osteoblasts/stromal cells.^{3,4} Sequentially, RANKL triggers osteoclastogenesis through RANK on preosteoclast cells. Acting as a soluble decoy receptor, OPG binds to RANKL and inhibits osteoclast development. Several studies have shown the opposing effects of RANKL and OPG on bone turnover. Genetic ablation of RANKL in mice results in osteopetrosis,^{5,6} whereas genetic deletion of OPG in mice results in high bone turnover and severe osteoporosis.⁷⁻⁹ Moreover, several factors initiating bone resorption not only upregulate RANKL expression but also inhibit OPG expression in osteoblasts/stromal cells.^{3,10} Upregulation of RANKL has also been seen in inflamed periodontal tissues, indicating that RANKL participates in the processes of periodontal tissue destruction.^{11,12} On the other hand, the RANKL/OPG ratio is increased in periodontitis compared to non-diseased individuals, suggesting that this molecular interaction may be important in modulating local bone loss. The RANKL/OPG ratio was found to be significantly increased in gingival crevicular fluid (GCF) of patients with periodontitis compared to healthy individuals.¹³

As a therapeutic drug for preventing bone loss, OPG has recently been evaluated in preclinical studies relating to estrogen deficiency, skeletal tumors, and specific cancers,^{6,14-17} as well as in clinical trials involving postmenopausal women, juvenile Paget's disease, and lytic bone disease associated with cancer.¹⁸⁻²⁰ All of these results showed that OPG has significant effects on the inhibition of bone loss.

The use of OPG as an inhibitor of alveolar bone destruction in periodontal disease was studied in mice orally infected with *Actinobacillus actinomycetencomitans*. Inhibition of RANKL function with OPG treatment significantly reduced the number of osteoclasts and alveolar bone loss.^{21,22}

The aim of this study was to evaluate the therapeutic effects of human recombinant OPG fusion protein (rhOPG-Fc) on preventing alveolar bone loss in an acute model of ligature-induced experimental periodontitis as assessed histologically and morphometrically.

MATERIALS AND METHODS

Experimental Design

All animal experiment procedures in this study were approved by the University of Michigan Committee of Use and Care of Animals.

To explore the OPG-Fc effects on alveolar bone loss in experimental periodontitis, 32 male Sprague-Dawley rats^{||} (weight: 250 to 300 g) were divided into

four experimental groups: group A, animals receiving no treatment (normal healthy control or NT); group B, animals receiving rhOPG-Fc[¶] subcutaneous administration twice weekly (OPG-treated healthy controls or OPG alone group); group C, animals exposed to disease induction and OPG subcutaneous injection twice weekly (OPG-treated diseased animals); and group D, animals exposed to disease induction and subcutaneous vehicle administration twice weekly (vehicle-treated diseased animals). There were four animals at each designated time point for each group. Block biopsies were harvested at 3 and 6 weeks after disease induction and/or OPG administration.

To further study the in vivo pharmacokinetics of injected rhOPG-Fc, four normal healthy animals received a single subcutaneous administration of rhOPG-Fc, and serum rhOPG-Fc was measured by an enzyme-linked immunosorbent assay (ELISA) at designated time points.

Experimental Periodontal Disease Induction and OPG Administration

Sprague-Dawley rats were anesthetized using inhalation anesthesia with isoflurane. 3/0 cotton ligatures were placed bilaterally into the gingival sulci of the mandibular first molar teeth. The ligatures were evaluated twice weekly, gently displaced apically into the gingival sulci to ensure a subgingival position, and replaced when necessary. The use of ligatures for induction of experimental periodontitis elicits rapid alveolar bone destruction through two combined mechanisms: an inflammatory process induced by increased microbial biofilm formation around the cervix of the teeth and an acute physical irritation factor as a consequence of the subgingival placement of the ligature, typically leading to the loss of approximately one-half of the bone support over a period of 3 to 6 weeks. The rhOPG-Fc was administered subcutaneously at a dose of 10 mg/kg animal body weight twice a week during 3 or 6 weeks.

In Vivo Pharmacokinetics of Injected rhOPG-Fc

To study the pharmacokinetics of a single subcutaneous injection of rhOPG-Fc at a dose of 10 mg/kg rat body weight, ~600 μ l blood was drawn from the tail vein of each animal at 0, 0.5, 1, 3, 7, 14, and 21 days. The samples were transferred into serum separator tubes[#] and centrifuged at 4,000 rpm for 10 minutes at 4°C. The supernatants were collected and stored at -80°C until needed for analysis. The content of serum rhOPG-Fc was measured using a commercially available human OPG ELISA kit.** The ELISA

^{||} Harlan, Indianapolis, IN.

[¶] Amgen, Thousand Oaks, CA.

[#] Becton Dickinson, Franklin Lakes, NY.

** American Laboratory, Windham, NH.

procedures were performed according to the manufacturer's instructions.

Serum rhOPG-Fc and Tartrate-Resistant Acid Phosphatase-5b (TRAP-5b) Measurements During Disease Progression

To measure rhOPG-Fc serum concentration after twice weekly OPG injections as a part of the experimental protocol, the blood from the tail vein was drawn at 0, 1.5, 3, 4.5, and 6 weeks, and serum was collected according to the methods outlined above.

Serum rhOPG-Fc and TRAP-5b levels were measured by commercially available human OPG^{††} and rat TRAP-5b^{‡‡} ELISA kits, respectively. The ELISA procedures were performed according to the manufacturer's instructions.

OPG-Fc Clearance From Bone

Young male rats were injected once (intravenously [IV]) with rhOPG-Fc at 5 mg/kg. Groups of rats (N = 6) were sacrificed at various times after treatment. Histologic sections of the proximal tibial metaphysis were subjected to immunohistochemistry analysis for human Fc (immunoglobulin [IgG]^{§§}). Deparaffinized 4- μ m sections were blocked,^{§§} and sections were incubated with rabbit anti-human IgG^{|||} at 1:4,000 for 1 hour. Antibody was detected by biotinylated goat anti-rabbit IgG^{¶¶} and followed with alkaline phosphatase ABC complex.^{##} The reaction was visualized with red alkaline phosphatase substrate.^{***} All sections were counterstained with hematoxylin.

Microcomputed Tomography (μ CT) Scanning and Analysis

In vitro μ CT provides high qualification and accurate quantification of mineralized tissues such as alveolar bone and teeth.²³ Each mandibular specimen was scanned and reconstructed at 18 \times 18 \times 18- μ m voxels using a μ CT system.^{†††} A three-dimensional (3-D) volume viewer and analyzer software^{‡‡‡} were used as the tool for both 3-D and 2-D visualization and quantification.

Linear and volumetric analyses were based on a previously developed methodology.²³ In brief, vertical, linear bone loss was obtained by measuring the distance from the cemento-enamel junction (CEJ) to the alveolar bone crest or to the base of the alveolar intrabony defect at the mesial surface of the mandibular first molar teeth. In terms of 3-D analysis, the most mesial root of the first molar (m-M1), the second molar (m-M2), the roof of the furcation, and root apex of M1 were used as reproducible landmarks for estimation of alveolar bone loss. Two-dimensional regions of interest (ROIs) were drawn at regular intervals (average, eight data slices) on a coronal view and reconstructed as a 3-D structure to quantify volumetric parameters, bone volume fraction (BVF), and bone

mineral density (BMD; mg/cc). The measurements of coded specimens were made by two independent, calibrated examiners (JAC and CHP).

Histology and TRAP Immunostaining

TRAP immunohistochemical staining was performed to identify and quantify osteoclast-like cells. Harvested mandibulae were fixed for 48 hours in 10% neutral-buffered formalin, decalcified with 10% EDTA for 2 weeks, embedded in paraffin, and cut into 4- to 5- μ m-thick sections. TRAP immunohistochemical staining was performed on these sections with anti-TRAP antibody^{§§§} and an immunostaining kit^{|||} to identify osteoclast-like cells covering the bone surface.

Images of coded specimens were captured using a microscope^{¶¶¶} fitted with a digital camera^{###} for analysis using software.^{****} The length of the bone surface covered by osteoclasts in a 0.5-mm coronal ROI at the alveolar crestal bone was measured by a single calibrated examiner (QJ).

Statistical Analysis

The differences among groups for linear and volumetric bone loss measurements, serum level of rhOPG-Fc and TRAP5b, and osteoclast-like cell surface area were statistically assessed by one-way analysis of variation (ANOVA) with Tukey multiple comparison post hoc test using a statistical software package.^{††††} The level of significance was set as $P \leq 0.05$.

RESULTS

In Vivo rhOPG-Fc Pharmacokinetics

The healthy animals receiving a single injection of rhOPG-Fc displayed an increase in serum rhOPG within 12 hours after administration, reaching a maximal level of 23.2 ± 5.1 μ g/ml at 3 days. Serum rhOPG subsequently decreased to 1.2 ± 1.4 μ g/ml at 14 days and 0.125 ± 0.152 μ g/ml at 21 days (Fig. 1).

OPG-Fc Clearance From the Vasculature of Rat Bone

After IV injection of human OPG-Fc, OPG primarily was circulated in blood rather than in the bone matrix. At 12 hours after administration, the peak level of serum OPG was reached and subsequently decreased

†† ALPCO Diagnostics, Salem, NH.

‡‡ RatTRAP Assay, SBA Sciences, Oulu, Finland.

§§ CAS Block, Zymed Laboratories, San Francisco, CA.

||| Jackson Laboratories, West Grove, PA.

¶¶ Vector Laboratories, Burlingame, CA.

Vector Laboratories.

*** Vector Laboratories.

††† GE Healthcare, London, ON.

‡‡‡ Microview Analysis+ v.2.1.2 software, GE Healthcare, London, ON.

§§§ sc-30833, Santa Cruz Biotechnology, Santa Cruz, CA.

||| Goat ABC Staining System kit (sc-2023), Santa Cruz Biotechnology.

¶¶¶ Eclipse 50i, Nikon, Melville, NY.

Digital Sight DS U1, Nikon.

**** Image Pro Plus, Media Cybernetics, Silver Spring, MD.

†††† GraphPad Prism version 4.00, GraphPad Software, San Diego, CA.

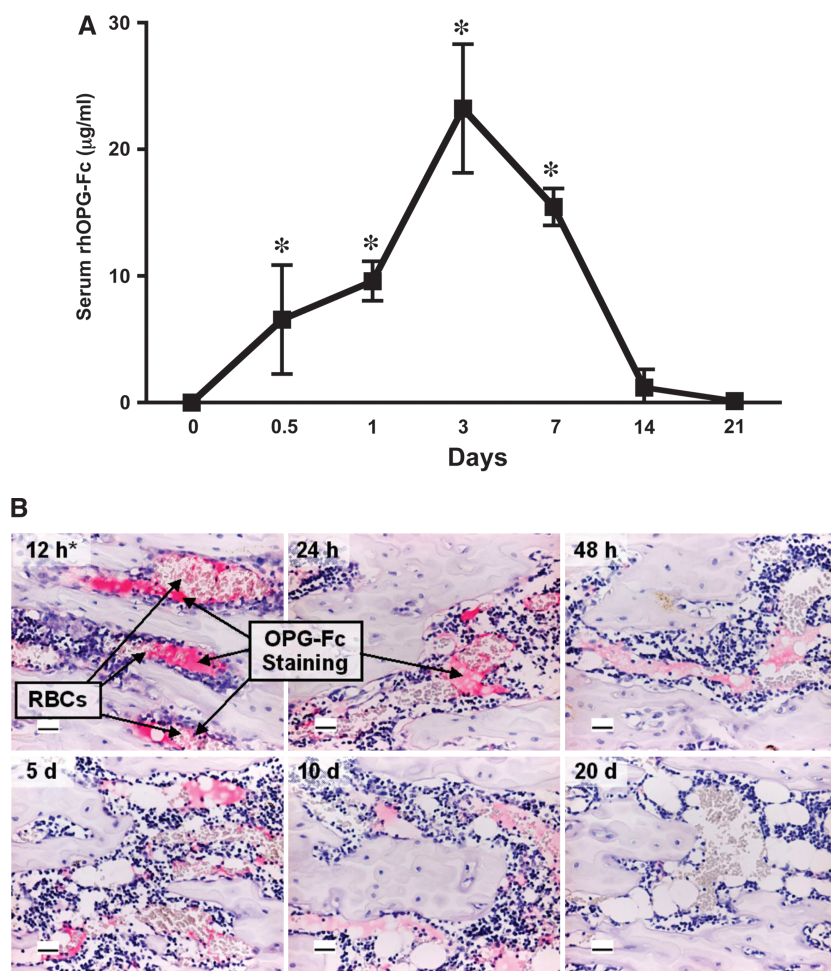


Figure 1.

In vivo rhOPG-Fc pharmacokinetics after a single subcutaneous administration. **A)** The maximum level of serum rhOPG was seen at 3 days after administration. Serum rhOPG decreased within 14 days. At 21 days after injection, the delivered rhOPG was eliminated completely. Bars represent SDs. * $P < 0.01$ compared to baseline. **B)** Human OPG immunostaining in the proximal tibial metaphysis. Young male rats received a single infusion IV with human OPG-Fc at 5 mg/kg. The delivered human OPG circulated primarily in the blood rather than integrating into the bone matrix. The highest serum level of administered human OPG appeared 12 hours after IV infusion, and the serum OPG was eliminated over time. $N = 6$ animals per group. Bars = 25 μm . RBCs = red blood cells; h = hours; d = days.

over time. At 20 days, no circulating OPG was found in the blood vessels of bone (Fig. 1B).

Serum rhOPG-Fc and TRAP-5b Levels During Disease Progression

Figure 2 shows serum rhOPG and TRAP-5b levels after rhOPG-Fc administration twice a week. By 10 days after injection, the serum rhOPG levels of OPG-treated healthy and diseased animals rose sharply to $31.6 \pm 12.3 \mu\text{g/ml}$ and $34 \pm 28.4 \mu\text{g/ml}$, respectively. The serum OPG within the OPG-treated diseased animals steadily increased over 6 weeks, whereas the serum OPG level within the OPG-treated healthy control showed no changes through 6 weeks. At 6 weeks, the OPG levels in OPG-treated diseased animals were sig-

nificantly greater than the OPG-treated healthy controls ($P < 0.01$). Compared to the vehicle-treated diseased animals, OPG levels of OPG-treated animals were significantly higher at each designated time point ($P < 0.01$; Fig. 2A). The endogenous OPG levels in normal healthy controls and vehicle-treated animals were low (data not shown).

The changes in serum TRAP-5b levels within the rhOPG-Fc-injected and non-rhOPG-Fc-injected animals are shown in Fig. 2B. During the first 10 days after rhOPG-Fc administration, serum TRAP-5b levels in rhOPG-Fc-injected animals sharply declined to undetectable levels, whereas TRAP-5b levels in non-rhOPG-Fc-treated animals decreased only slightly or remained unchanged. After 10 days, the serum TRAP-5b levels of rhOPG-Fc-treated animals sustained lower levels, but the serum TRAP-5b levels of non-rhOPG-Fc-treated animals slowly decreased. At all time points except baseline, the TRAP-5b levels in rhOPG-Fc-delivered animals were significantly lower than those of non-rhOPG-Fc-injected animals ($P < 0.01$). No other groups displayed differences in TRAP-5b levels (Fig. 2B).

μCT Analysis

The alveolar bone crest at 3 weeks within the vehicle-treated animals significantly decreased from $0.83 \pm 0.1 \text{ mm}$ (no treatment group) to $1.28 \pm 0.2 \text{ mm}$, which indicates that ~50% bone loss was elicited by experimental periodontitis (Figs. 3 and 4A). At 6 weeks, the bone crest within the vehicle-treated animals also decreased from $1.05 \pm 0.1 \text{ mm}$ (no treatment group) to $1.4 \pm 0.2 \text{ mm}$, resulting in 40% bone loss. Significant differences of CEJ to bone crest (C-C) distance were only found in the vehicle-treated animals compared to the other three groups.

For volumetric measurements at the 3-week time point, experimental periodontitis resulted in the lowest BVF in the vehicle-treated animals compared to the other three groups, whereas the OPG-treated healthy controls had the highest BVF (Fig. 4B). At 6 weeks, the vehicle-treated animals again showed the lowest BVF among all groups, whereas the OPG administration groups had significantly higher BVF compared to the no treatment group (Fig. 4B). In terms of BMD, the OPG-treated healthy controls

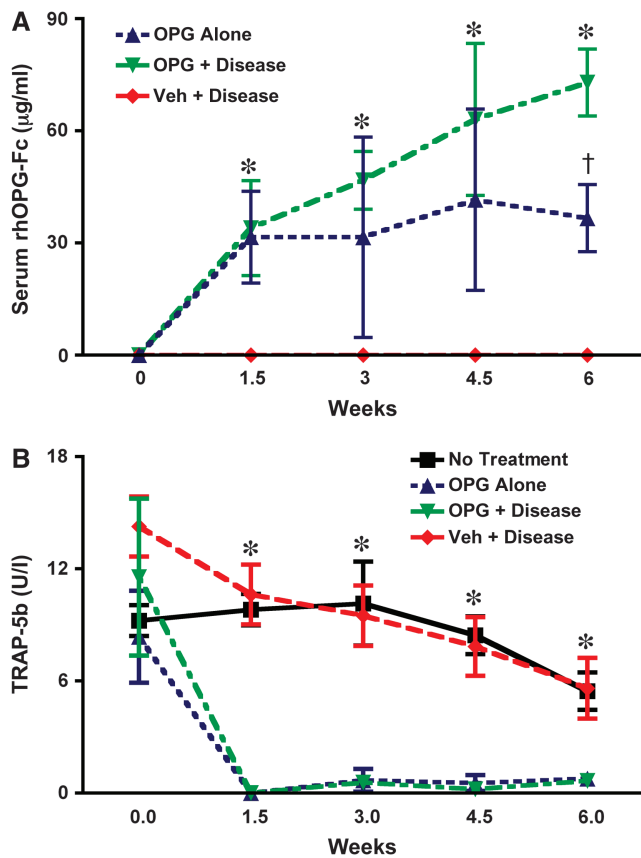


Figure 2.

A) Serum rhOPG levels after twice weekly subcutaneous administration. Higher serum rhOPG levels were seen in OPG delivery groups, whereas rhOPG levels remained almost undetectable in vehicle-treated animals. At 6 weeks, the serum rhOPG levels between the OPG + disease and the OPG alone groups were statistically significantly different ($^{\dagger}P < 0.05$). * $P < 0.05$ compared to the vehicle group. Bars represent SDs. **B)** Serum TRAP-5b levels after repeated subcutaneous administration. Serum TRAP-5b levels in rhOPG-injected animals decreased sharply at 10 days and remained very low until 6 weeks, whereas the serum TRAP-5b levels in non-rhOPG-injected animals gradually declined. Except at baseline, the TRAP-5b levels in non-rhOPG-treated groups were significantly higher than those in rhOPG-injected groups. * $P < 0.05$ compared to non-rhOPG-treated groups. Bars represent SDs. $N = 4$ animals per group. Veh = vehicle.

showed the highest BMD, whereas the vehicle-treated animals had the lowest BMD at 3 weeks. At 6 weeks, the vehicle-treated animals had the lowest BMD, and there was a significant difference found between the normal healthy and OPG-treated healthy controls (Fig. 4C).

TRAP Immunostaining and Osteoclast Surface Analysis of Alveolar Bone

Histologic analysis of four animals in each group at 3 and 6 weeks revealed increases in TRAP-stained osteoclasts in the region of the alveolar bone crest in diseased vehicle-treated animals compared to healthy controls (Fig. 3). In accordance with histologic obser-

variations, the coverage of osteoclasts at the alveolar bone crest showed that osteoclasts in vehicle-treated animals occupied ~50% the surface of the alveolar bone within the coronal 0.5 mm, which was the highest of all the groups (Fig. 5). In contrast, very few TRAP-stained osteoclasts were observed in OPG-treated animals. OPG treatment of healthy animals was associated with a virtual absence of osteoclasts along the alveolar bone crest, whereas OPG treatment of diseased animals resulted in a three-fold reduction in osteoclast surface compared to vehicle-treated diseased animals (Fig. 5). This level of suppression reduced osteoclast surface area to levels found in normal healthy animals. In addition, compared to the linear bone loss measurement, the bone loss is related to the osteoclast surface area covering the bone (Fig. 5). The vehicle-treated diseased animals showed the highest osteoclast coverage and the most extensive bone loss.

DISCUSSION

To the best of our knowledge, this study showed for the first time a protective effect of OPG in an acute model of experimental periodontitis. To evaluate the effect of human OPG on the alveolar bone changes of rats at physiologic and pathologic conditions, it is imperative to show adequate systemic drug exposure. Human proteins including OPG-Fc can be immunogenic in rats, which would lead to rapid clearance of the drug and inadequate drug exposure. Single-dose pharmacokinetic assessment of human OPG-Fc revealed a C_{max} at day 3, which indicates that twice-weekly administrations would ensure maximal exposure. After twice-weekly OPG administration, $>30 \mu\text{g/ml}$ serum OPG concentration was obtained and sustained, which proved to be the effective serum OPG level to reduce the number of osteoclasts and inhibit bone loss (Figs. 4 and 5). This serum OPG concentration is similar to the serum OPG level ($26.1 \pm 5.2 \mu\text{g/ml}$) found to be optimal for preventing bone resorption as previously reported by Capparelli et al.²⁴ However, inflammation may influence in vivo OPG degradation. Serum OPG levels in OPG-treated diseased animals remained elevated and were two-fold higher at 6 weeks compared to the OPG alone group, which may result from the decrease of the OPG degradation-related enzymes elicited by periodontal inflammation.

Three-dimensional images of the mandibular molars generated by μCT were used to evaluate the preventive effects of OPG on alveolar bone loss. Linear measurements indicated that the vehicle-treated animals displayed higher levels of bone loss compared to other groups, whereas both groups receiving OPG injection showed similar bone levels compared to the healthy controls. This suggests that OPG inhibits

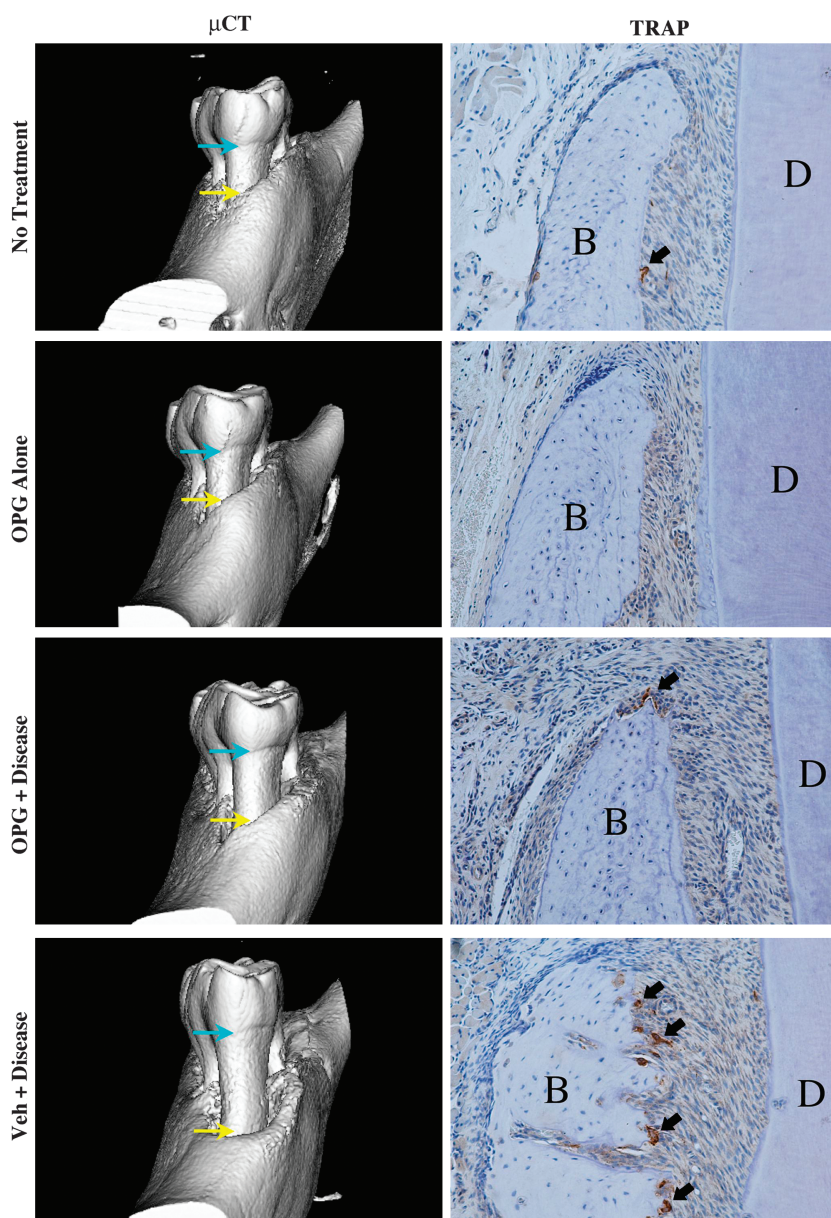


Figure 3.

OPG-Fc blocks alveolar bone loss in experimental periodontitis. Left panels show the mesial view of μ CT 3-D images of mandibular first molars of each group at 3 weeks. The vehicle + disease group shows the greatest degree of bone loss. Right panels show the histology of the alveolar bone at the mesial side of mandibular first molars of each group at 3 weeks (TRAP immunostaining; magnification, $\times 200$). TRAP-positive osteoclasts are stained brown. Higher numbers of positively stained osteoclasts were noted on the surface of alveolar bone in the vehicle + disease groups. Few osteoclasts were seen at the alveolar bone crest in the OPG + disease group. Furthermore, no positively stained cells were found in the OPG alone group. Blue arrows demarcate the CEJ. Yellow arrows indicate the alveolar bone crest. Black arrows indicate positive TRAP-stained osteoclast-like cells. Veh = vehicle; B = bone crest; D = dentin. N = 4 animals per group.

alveolar bone loss induced by experimental periodontitis. Protective effects of OPG on alveolar bone resorption were previously shown in an *A. actinomycetemcomitans* oral inoculation-induced periodontitis model^{21,22} and a tooth biomechanical movement

model (our unpublished data). In addition, measurements of the BVF, representing the percentage of bone volume of the delineated region, were statistically lower in the vehicle-treated animals compared to all other groups at 3 and 6 weeks, showing that experimental periodontitis stimulated more bone loss in the absence of OPG administration. Therefore, OPG seems to rescue not only alveolar bone height but also loss of BMD induced by experimental periodontitis.

To evaluate the effects of OPG on the osteoclast formation in alveolar bone, the coronal 0.5 mm of bone crest at the mesial surface of the first molars was chosen because those areas are under the direct influence of experimental periodontitis and most subject to osteoclast formation. Our results showed that the vehicle-treated diseased animals showed a higher percentage of bone surface covered by TRAP-positive osteoclasts than the other groups at 3 weeks, whereas the OPG-treated diseased animals had the same bone surface coverage of TRAP-positive osteoclasts as normal rats, which suggests that OPG inhibits osteoclast formation. Similar results were also seen in the application of OPG to situations of increased osteoclastic bone resorption, which results from certain types of cancers, rheumatoid arthritis,²⁵ or *A. actinomycetemcomitans* inoculation.^{21,22} In addition, OPG administration also causes a decrease in serum TRAP-5b, a marker of osteoclastic resorption.²⁶ This indicates that the reduction of osteoclast number elicited by OPG application results in a decrease of TRAP-5b originating from osteoclasts.

A potentially important advantage for clinical application of OPG is the lack of incorporation of OPG into bone matrix, as shown in Fig. 1B. As a result, its effects on osteoclasts and bone remodeling are fully reversible.^{24,27} This mechanism of action could have benefits versus agents such as bisphosphonates, which are directly incorporated into bone matrix and thus have poor reversibility. Bisphosphonates have shown efficacy in patients with osteoporosis, Paget's disease, and tumor bone disease,²⁸ and these agents have shown potent effects as host-modulating

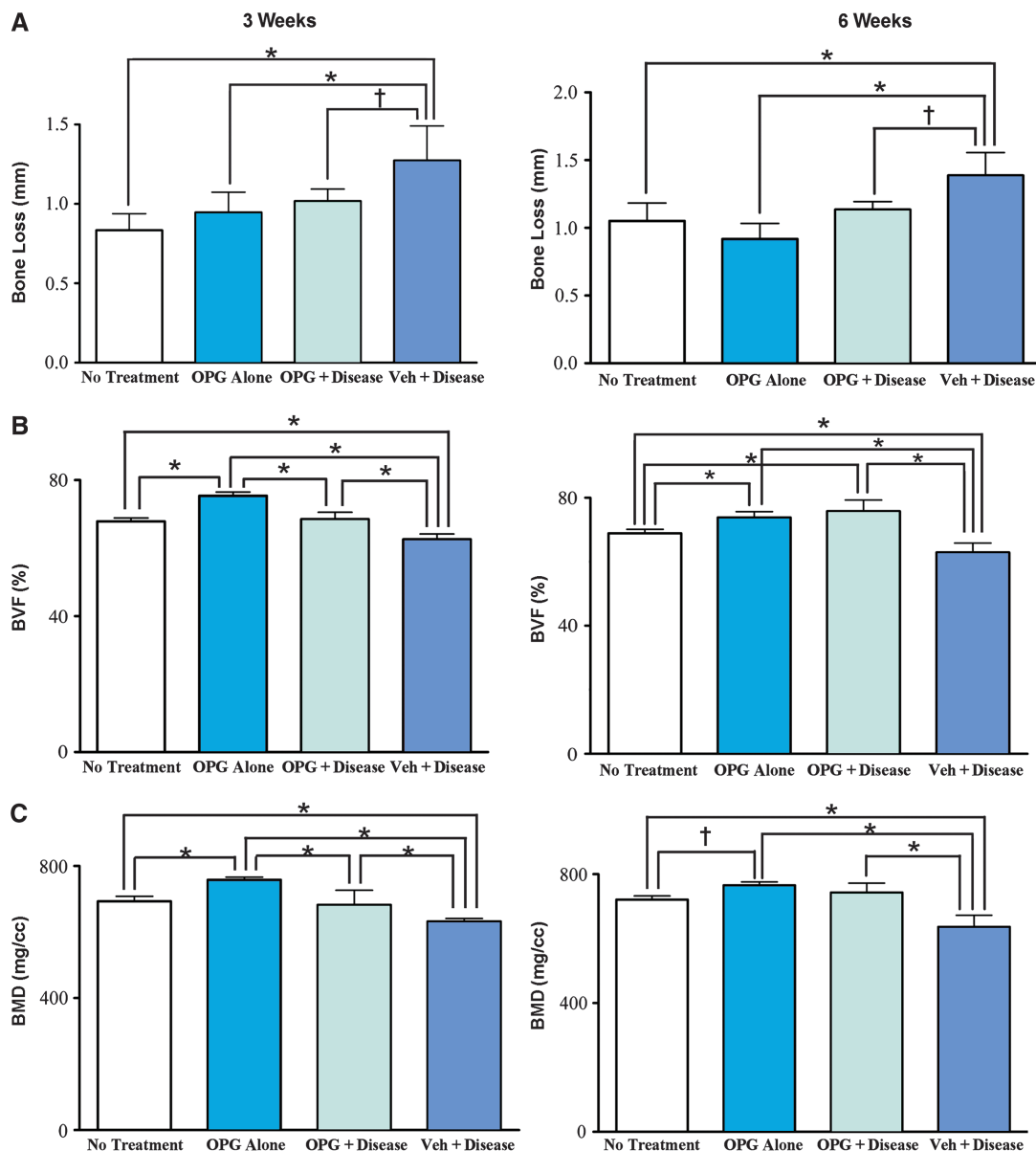


Figure 4.

OPG-Fc blocks alveolar bone loss in experimental periodontitis as measured by linear and volumetric μ CT. **A)** The linear measurement of the distance from the CEJ to alveolar bone crest at the mesial roots of mandibular first molars in each group. The greatest difference was seen in the vehicle + disease group at both 3 and 6 weeks, whereas there was no significant difference among other groups. **B)** The fractions of bone volume versus the total volume surrounded by the superficial surfaces of five roots of first mandibular molar. At 3 and 6 weeks, the vehicle + disease group showed the smallest BVF, whereas the OPG alone group displayed the greatest BVF. No significant difference was found between the no treatment and OPG + disease groups. **C)** BMD for the regions surrounded by the superficial surfaces of all roots of first mandibular molars of each group. At 3 and 6 weeks, BMD in the vehicle + disease group was the lowest, whereas the OPG alone group displayed the highest BMD. No significant difference was found between no treatment and OPG + disease groups. $N = 4$ animals per group. * $P < 0.05$; † $P < 0.01$; bars represent SDs. Veh = vehicle.

agents for periodontal disease treatment.²⁹⁻³¹ However, bisphosphonate therapy has also been associated with osteonecrosis of the jaw (ONJ),^{32,33} a condition described by the persistent exposure of necrotic bone in the oral cavity. The etiology of bisphosphonate-related ONJ is poorly understood, but periodontal disease has been the most common comorbidity in bisphosphonate-treated patients with

ONJ.³² In cancer patients on IV bisphosphonates, the relative risk of developing ONJ increases markedly after several years of bisphosphonate use.³³ Bisphosphonate accumulation in bone matrix is a direct function of the total administered dose,³⁴ and the skeletal uptake of bisphosphonates is not reduced by prior high-dose bisphosphonate therapy.³⁵ These observations suggest that skeletal accumulation of

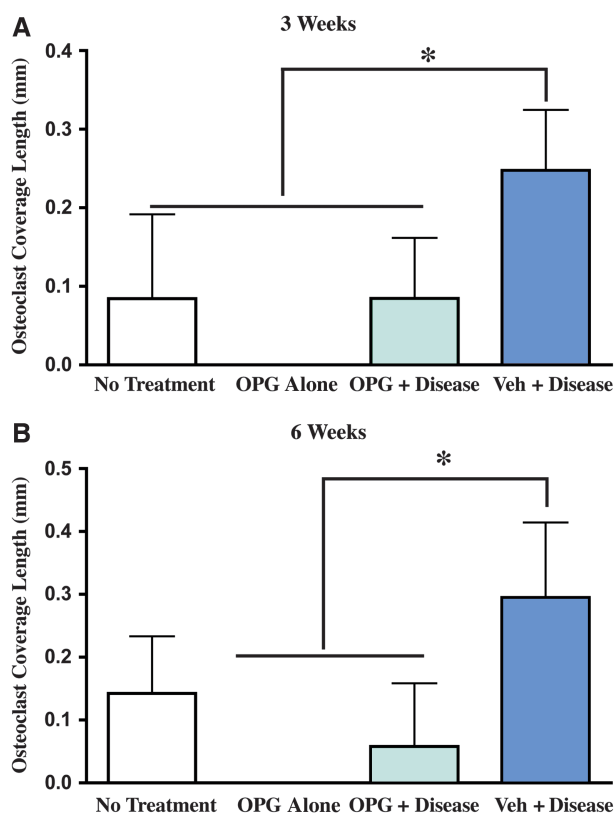


Figure 5.

OPG administration inhibits osteoclast formation at the alveolar bone crest in experimental periodontitis. The osteoclast surface coverage at the coronal 0.5-mm region of interest in alveolar bone at the mesial of the mandibular first molars was evaluated histomorphometrically at 3 and 6 weeks using TRAP immunostaining. At 3 weeks, osteoclast coverage area was the greatest in the vehicle + disease group, whereas there were no significant differences noted among the other three groups. At 6 weeks, the vehicle + disease group had the greatest osteoclast coverage at the alveolar crest compared to OPG administration groups, with no significant difference with the no treatment group. * $P < 0.05$. $N = 4$ animals per group. Veh = vehicle.

bisphosphonates continues despite the ability of these agents to markedly suppress bone turnover. Because periodontitis can be a chronic disease, it may be inappropriate to use long-term bisphosphonates for the prevention of alveolar bone loss until the etiology of bisphosphonate-related ONJ is elucidated.

CONCLUSIONS

In this study, OPG revealed strong preventive effects on alveolar bone loss in experimental periodontitis, thus showing promising therapeutic potential of OPG for treatment of periodontal disease. Future studies will need to examine the ability of OPG to block progression of established disease and human application.

ACKNOWLEDGMENTS

This study was supported by the National Institutes of Health (grant P30-AR46024), National Institute of

Dental and Craniofacial Research (DE 13397), and Amgen. The authors thank Stephen Adamu, senior research associate, Sheila Scully, director, and Gwyneth Van, scientist, from Amgen for performing the TRAP-5b ELISA assays and human OPG immunostaining. Dr. Paul J. Kostenuik is research scientist group leader of metabolic disorders research at Amgen. Qiming Jin and Joni A. Cirelli contributed equally to this work.

REFERENCES

- Page RC, Kornman KS. The pathogenesis of human periodontitis: An introduction. *Periodontol* 2000 1997;14: 9-11.
- Kirkwood KL, Cirelli J, Rogers J, Giannobile WV. Novel host response therapeutic approaches to treat periodontal diseases. *Periodontol* 2000 2007;43:294-315.
- Hofbauer LC, Khosla S, Dunstan CR, Lacey DL, Boyle WJ, Riggs BL. The roles of osteoprotegerin and osteoprotegerin ligand in the paracrine regulation of bone resorption. *J Bone Miner Res* 2000;15:2-12.
- Nakashima T, Kobayashi Y, Yamasaki S, et al. Protein expression and functional difference of membrane-bound and soluble receptor activator of NF-kappaB ligand: Modulation of the expression by osteotropic factors and cytokines. *Biochem Biophys Res Commun* 2000;275:768-775.
- Kong YY, Yoshida H, Sarosi I, et al. OPGL is a key regulator of osteoclastogenesis, lymphocyte development and lymph-node organogenesis. *Nature* 1999;397: 315-323.
- Simonet WS, Lacey DL, Dunstan CR, et al. Osteoprotegerin: A novel secreted protein involved in the regulation of bone density. *Cell* 1997;89:309-319.
- Bucay N, Sarosi I, Dunstan CR, et al. Osteoprotegerin-deficient mice develop early onset osteoporosis and arterial calcification. *Genes Dev* 1998;12:1260-1268.
- Mizuno A, Amizuka N, Irie K, et al. Severe osteoporosis in mice lacking osteoclastogenesis inhibitory factor/osteoprotegerin. *Biochem Biophys Res Commun* 1998; 247:610-615.
- Udagawa N, Takahashi N, Yasuda H, et al. Osteoprotegerin produced by osteoblasts is an important regulator in osteoclast development and function. *Endocrinology* 2000;141:3478-3484.
- Hasegawa T, Yoshimura Y, Kikui T, et al. Expression of receptor activator of NF-kappa B ligand and osteoprotegerin in culture of human periodontal ligament cells. *J Periodontal Res* 2002;37:405-411.
- Liu D, Xu JK, Figliomeni L, et al. Expression of RANKL and OPG mRNA in periodontal disease: Possible involvement in bone destruction. *Int J Mol Med* 2003;11:17-21.
- Crotti T, Smith MD, Hirsch R, et al. Receptor activator NF kappaB ligand (RANKL) and osteoprotegerin (OPG) protein expression in periodontitis. *J Periodontal Res* 2003;38:380-387.
- Mogi M, Otogoto J, Ota N, Togari A. Differential expression of RANKL and osteoprotegerin in gingival crevicular fluid of patients with periodontitis. *J Dent Res* 2004;83:166-169.
- Morony S, Capparelli C, Sarosi I, Lacey DL, Dunstan CR, Kostenuik PJ. Osteoprotegerin inhibits osteolysis and decreases skeletal tumor burden in syngeneic and nude mouse models of experimental bone metastasis. *Cancer Res* 2001;61:4432-4436.

15. Zhang J, Dai J, Qi Y, et al. Osteoprotegerin inhibits prostate cancer-induced osteoclastogenesis and prevents prostate tumor growth in the bone. *J Clin Invest* 2001;107:1235-1244.
16. Capparelli C, Kostenuik PJ, Morony S, et al. Osteoprotegerin prevents and reverses hypercalcemia in a murine model of humoral hypercalcemia of malignancy. *Cancer Res* 2000;60:783-787.
17. Oyajobi BO, Anderson DM, Traianedes K, Williams BJ, Yoneda T, Mundy GR. Therapeutic efficacy of a soluble receptor activator of nuclear factor kappaB-IgG Fc fusion protein in suppressing bone resorption and hypercalcemia in a model of humoral hypercalcemia of malignancy. *Cancer Res* 2001;61:2572-2578.
18. Bekker PJ, Holloway D, Nakanishi A, Arrighi M, Leese PT, Dunstan CR. The effect of a single dose of osteoprotegerin in postmenopausal women. *J Bone Miner Res* 2001;16:348-360.
19. Body JJ, Greipp P, Coleman RE, et al. A phase I study of AMG-0007, a recombinant osteoprotegerin construct, in patients with multiple myeloma or breast carcinoma related bone metastases. *Cancer* 2003;97:887-892.
20. Cundy T, Davidson J, Rutland MD, Stewart C, DePaoli AM. Recombinant osteoprotegerin for juvenile Paget's disease. *N Engl J Med* 2005;353:918-923.
21. Teng YT, Nguyen H, Gao X, et al. Functional human T-cell immunity and osteoprotegerin ligand control alveolar bone destruction in periodontal infection. *J Clin Invest* 2000;106:R59-R67.
22. Mahamed DA, Marleau A, Alnaeeli M, et al. G(-) anaerobes-reactive CD4+ T-cells trigger RANKL-mediated enhanced alveolar bone loss in diabetic NOD mice. *Diabetes* 2005;54:1477-1486.
23. Park CH, Abramson Z, Taba M Jr., et al. 3-D micro-CT image analysis of alveolar bone resorption and repair. *J Periodontol* 2007;78:273-281.
24. Capparelli C, Morony S, Warmington K, et al. Sustained antiresorptive effects after a single treatment with human recombinant osteoprotegerin (OPG): A pharmacodynamic and pharmacokinetic analysis in rats. *J Bone Miner Res* 2003;18:852-858.
25. Romas E, Sims NA, Hards DK, et al. Osteoprotegerin reduces osteoclast numbers and prevents bone erosion in collagen-induced arthritis. *Am J Pathol* 2002;161:1419-1427.
26. Halleen JM. Tartrate-resistant acid phosphatase 5B is a specific and sensitive marker of bone resorption. *Anticancer Res* 2003;23:1027-1029.
27. Kostenuik PJ. Osteoprotegerin and RANKL regulate bone resorption, density, geometry and strength. *Curr Opin Pharmacol* 2005;5:618-625.
28. Fleisch H. Bisphosphonates: Mechanisms of action and clinical use in osteoporosis – An update. *Horm Metab Res* 1997;29:145-150.
29. Lane N, Armitage GC, Loomer P, et al. Bisphosphonate therapy improves the outcome of conventional periodontal treatment: Results of a 12-month, randomized, placebo-controlled study. *J Periodontol* 2005;76:1113-1122.
30. Rocha M, Nava LE, Vazquez de la Torre C, Sanchez-Marin FJ, Garay-Sevilla ME, Malacara JM. Clinical and radiological improvement of periodontal disease in patients with type 2 diabetes mellitus treated with alendronate: A randomized, placebo-controlled trial. *J Periodontol* 2001;72:204-209.
31. Rocha ML, Malacara JM, Sanchez-Marin FJ, Vazquez de la Torre CJ, Fajardo ME. Effect of alendronate on periodontal disease in postmenopausal women: A randomized placebo-controlled trial. *J Periodontol* 2004;75:1579-1585.
32. Marx RE, Sawatari Y, Fortin M, Broumand V. Bisphosphonate-induced exposed bone (osteonecrosis/osteopetrosis) of the jaws: Risk factors, recognition, prevention, and treatment. *J Oral Maxillofac Surg* 2005;63:1567-1575.
33. Bamias A, Kastiris E, Bamia C, et al. Osteonecrosis of the jaw in cancer after treatment with bisphosphonates: Incidence and risk factors. *J Clin Oncol* 2005;23:8580-8587.
34. Komatsubara S, Mori S, Mashiba T, et al. Long-term treatment of incadronate disodium accumulates microdamage but improves the trabecular bone microarchitecture in dog vertebra. *J Bone Miner Res* 2003;18:512-520.
35. Lin JH, Chen IW, Duggan DE. Effects of dose, sex, and age on the disposition of alendronate, a potent anti-osteolytic bisphosphonate, in rats. *Drug Metab Dispos* 1992;20:473-478.

Correspondence: Dr. William V. Giannobile, Michigan Center for Oral Health Research, University of Michigan Clinical Center, 24 Frank Lloyd Wright Dr., Lobby M, Box 422, Ann Arbor, MI 48106. Fax: 734/998-7228; e-mail: wgiannob@umich.edu.

Submitted February 1, 2007; accepted for publication March 2, 2007.